Published by
NIGERIAN SOCIETY OF PHYSICAL SCIENCES
Available online @ https://journal.nsps.org.ng/index.php/jnsps

J. Nig. Soc. Phys. Sci. 7 (2025) 2558

Journal of the Nigerian Society of Physical Sciences

Sustainable remediation of vancomycin polluted water using pyrolysis biochar of pressed oil palm fruit fibre

Abiodun Oluwatosin Adeoye*, Rukayat Oluwatobiloba Quadri, Olayide Samuel Lawal

[a]*Department of Chemistry, Federal University Oye-Ekiti, Ekiti State, Nigeria*

Abstract

Pharmaceutical effluents, especially antibiotics, have significantly contributed to aquatic pollution in recent times, which has called for a sustainable approach to their removal. Adsorption is an efficient process to remove antibiotics from water via the use of materials that could adhere to pollutants and enhance extraction. This study investigated the efficiency of the solid pyrolysis product of pressed palm oil fruit fibre by varying pH and temperature on the removal of vancomycin from water. The following models were used to describe the adsorption kinetics: pseudo-first order, pseudo-second order, Avrami, Elovich, and intraparticle diffusion model, while Temkin, Langmuir, Dubinin Radushkevich (D-R), and Freundlich were used to describe the isotherm. The highest value of the correlation coefficient (R^2) of 0.985 was obtained for the pseudo-first order kinetics model. At 40 °C, the correlation coefficients R^2 were 0.953, 0.995, 0.967, and 0.940 for Temkim, D-R, Langmuir, and Freundlich, respectively. The obtained ranges for standard Gibb's free energy (ΔG°) > −28.94 kJ/mol and the standard entropy (ΔS°) > 0 demonstrate that the adsorption of vancomycin is favourable and spontaneous. The adsorption process was mainly via a physical process, spontaneous and exothermic, since the standard enthalpy (ΔH°) is -13.92 kJ/mol. The maximum adsorption capacity at 40 °C using the Langmuir isotherm is 3.902 mg/g. The material is a potentially cheap, eco-friendly method for remediating vancomycin from water.

DOI:10.46481/jnsps.2025.2558

Keywords: Pyrolysis, Biochar, Antibiotics, Adsorption, Pollution

Article History :
Received: 04 December 2024
Received in revised form: 18 January 2025
Accepted for publication: 14 February 2025
Available online: 07 March 2025

Communicated by: B. J. Falaye

1. Introduction

The release of untreated water to nearby water bodies from pharmaceutical industries producing antibiotics has contributed on a large scale to aquatic ecosystem pollution. It has been a significant contention issue in recent years that has seriously drawn the attention of environmentalists in the field [1, 2]. Approximately 100,000 to 200,000 tons of antibiotics are produced annually, with a cumulative total exceeding one billion tons since 1940. Of this production, only 10% to 90% is metabolized by humans or animals, resulting in the excretion of active forms into nearby aquatic medium and terrestrial areas. This results in the accumulation of antibiotic concentrations, which over time presents a significant global health concern owing to evident pollution demonstrating the adverse effects of antibiotics on human health and the ecosystem [3, 4].

Vancomycin is a potent antibiotic for cases of severe bacterial infections such as septicaemia and endocarditis. Still, when released into water bodies, it becomes dangerous to the aquatic ecosystem, as shown in a case where it negatively impacts the

*Corresponding author: Tel. No.: +234-805-647-8597.
Email address: bioken2017@gmail.com (Abiodun Oluwatosin Adeoye)

development and reproductive functions of aquatic species, including zebra fish, underscoring its potential for biomagnification in aquatic food webs [5–7]. Its continuous presence in the ecosystem can result in the growth of microorganisms with resistant strains, thereby endangering public health. Vancomycin has become an indispensable antibiotic in medical therapy for gram-positive bacterial infections, a glycopeptide from Amycolatopsis orientalis, enduracididine, and an aglycon ring [8]. This molecule has detrimental adverse effects on aquatic habitats. It has proven to be resistant to biological and chemical degradation techniques, which cause an increase in its presence when released into the natural environment and then accumulate to cause toxicity in diverse settings due to its extended half-life and slow, gradual degradation [9–13]. It has been widely accepted as an antibiotic due to its inherent properties, such as cell wall formation inhibition, tempering with gene expression, and the potential to inactivate the target bacterial enzymes. Its wide use is due to its high superiority in protein targeting compared to peptide nucleic acids [8]. Even in a system where it was not a threat from pharmaceutical effluents, its residues can also be found in urine and faeces, which could, therefore, contaminate nearby water bodies in a system of open excretion and some of it entering urban wastewater systems [14, 15]. Some previous analyses indicated that more than 90% of given vancomycin is excreted via renal routes [6, 7, 16, 17].

Biochar is a solid product of the pyrolysis of biomass wastes with adequate surface area, a porous architecture, and high adsorption capacity to remove pollutants. It has additional benefits, such as soil enhancement and carbon sequestration potential [18]. The pyrolysis temperature of biomass waste to form biochar has a strong effect on the pollutant adsorption mechanism because adsorption to different layers or subdomains of the biochar can be governed by linear and nonlinear mechanisms [19].

Adsorption is an efficient process to remove contaminants from water via the use of compounds or materials that could adhere to pollutants and enhance extraction. The adsorption of target pollutants (vancomycin) to the pyrolytic biochar surface occurs via weak electrical force interactions between the adsorbate and biochar surface or through partitioning of vancomycin molecules between the solid adsorbent and water, a process termed physical adsorption [8]. The process can be either attractive or repulsive. Physical adsorptions are reversible reactions with a slower rate when compared to chemical adsorption and are affected by factors that include temperature and pH [8, 20]. This phenomenon is shown in the adsorption isotherm, where mass fractions are obtained from the biochar mass (mg) relative to the vancomycin solution volume (L). The amount of antibiotics removed by biochar depends on its surface area and pore structure. The larger the surface area, the higher the amount of antibiotics that will be removed since a larger surface area facilitates adsorption both on the surface and within biochar pores, accessing various transition sites, including meso, micro, and macro pores. Also, factors to include are the hydrophilicity or hydrophobicity of biochar, which affects adsorption efficiency [21, 22]. In chemical adsorption, an irreversible bond is formed between adsorbate and adsorbent. The chemical adsorption driving forces largely depend on common functional groups (-OH, -COOH, and -C=O) on the biochar surface, which contributes to the number of available functional groups that the adsorbate can bind with. Migration of pollutants to the internal surface areas is possible, making biochar a suitable pollutant remediation material. For a cationic antibiotic, it can be projected that the final removal of vancomycin will occur during diffusion through the biochar matrix as it reacts with these weak acid sites [8]. This mechanism of adsorption is affected by parameters of pH, temperature, ionic strength of the bulk solution, and aqueous chemistry.

The existing methods of water treatment techniques, such as membrane processes Cheng *et al*. [23], biodegradation Xu *et al*. [24], ozonation Bai *et al*. [25], Moreira *et al*. [26], irradiation using UV, chemical oxidants such as potassium ferrate and permanganate, which can generate hydroxyl (-OH) Niu *et al*. [27], de Lima Perini *et al*. [28], Demarchis *et al* [29] could achieve removal of 60-90% of antibiotics, leaving the remaining percentages depleted into the ecosystem [30, 31]. These techniques are also expensive and not totally eco-friendly. The use of chemicals such as ozone, trihalomethanes, and halogens could lead to toxicity [32, 33].

There are still existing issues of water contamination with antibiotics such as vancomycin, tetracycline, penicillin, ciprofloxacin, etc. [34]. Recently, the adsorption process has tended towards eco-friendly materials such as biomass waste, which are described as cheap and widely spread to encourage all-time availability across different geographical areas and do not produce secondary pollution [35, 36]. Previous studies have used activated carbon to remove antibiotics from aqueous medium, as reported in Legnoverde *et al*. [37], who used SBA-15 mesoporous silica to achieve increased cephalexin removal from aqueous solution, and Pouretedal and Sadegh [38], who used vine wood ash to remove antibiotics from aqueous medium. Activated carbon has a high adsorption capacity; they are mainly bioavailable [38]. However, the significant demerits associated with activated carbon for antibiotic remediation have to do with the separation from the aqueous solution after use due to their finest particle size and high dispersivity. Also, desorption of antibiotics from the activated carbon is likely in cases where direct water exposure occurred or in cases where a rapid change in the ambient liquid could affect interactions between adsorbent and adsorbate.

Biochar has been extensively reported to remove antibiotics in water [39–42]. A ton of fresh oil palm fruit bunch generates 130-150 kg of pressed oil palm fruit fibre Adeoye *et al* [43]. Hence, this current research seeks to improve the utilisation of pressed oil palm fruit fibre in Nigeria by not limiting it as a local material for only thermal energy but also using its biochar for vancomycin remediation.

2. Materials and methods

2.1. Chemicals

Raw antibiotic powder (vancomycin) used in this study was of analytical grade with a purity of 99.0% purchased from

Merck, formerly Sigma-Aldrich (UK). pH was adjusted using concentrated hydrochloric acid and sodium hydroxide (NaOH). The chemical structure of vancomycin hydrochloride has a molecular formula of $C_{66}H_{76}Cl_3N_9O_{24}$ and a molecular weight of 1485.73 g/mol. A vancomycin stock solution of 1000 mg/L was prepared by adding 100 mg to 100 mL of deionised H_2O in a beaker. The initial concentration of the study ranged from 5 mgL^{-1} to 25 mgL^{-1}, achieved through serial dilution. A laboratory refrigerator set at 4 °C was used to store the solution before experimentation.

2.2. Pyrolysis experiment

Pyrolytic solid biochar, derived from pressed oil palm fruit fibre seen in Figure 1 and pulverized to a particle size of 0.5 to 2 mm, was produced using a fixed bed pyrolyzer shown in Figure 2. A 2 kg mass of pressed oil palm fruit fibre was loaded in the 17.4 L fixed bed pyrolyzer purged with N_2 to create an inert environment and which was heated from room temperature of 25 ^{o}C to the set pyrolysis temperature varied between 350 to 650 ^{o}C as described in Adeoye *et al.* [44]. The reactor was allowed to cool to collect the resultant biochar and weigh it. The bio-oil component, a mixture of (aqueous and oil phases) was collected in the filtering flasks connected to the condensers and weighed. The pyrolysis gas yield was calculated as the difference between the total weight of loaded biomass and the summation of the weight of (biochar and bio-oil) expressed in percentage.

2.3. Characterization of biochar of pressed oil palm fruit fibre

A modern X-ray diffractometer manufactured by X'Pert, Philips, The Netherlands, at a rating of 4 x 10^3 V and 3.0 x 10^{-3} A, utilising CuK radiation at 1.5406 Å, operated at 2θ (5°–90°), gave information on the crystallinity component of the cellulose in pressed oil palm fruit fibre. The surface morphology of the pyrolysed pressed oil palm fruit fibre was investigated using scanning electron microscopy (SEM) with the trademark ThermoFisher-Scientific (Phenom ProX G5) operating at 10 KV. The elemental composition of the biochar in oxide form was determined using an XRF spectrometer with the trademark EulerX 900S. The surface area, pore volume and pore diameter were determined using BET Surface Area Analyzer - Quantachrome NOVA 2200E BET.

2.4. Batch experiments

The adsorption study of vancomycin onto the surfaces of the adsorbent was performed in a series of batch experiments under different input variables such as pH of the solution (3–11), contact time (5–360 min), adsorbent dosages of 0.1 g/40 ml, and initial antibiotic concentrations (5–25 mg/L). The mixture was stirred at 100 rpm on a thermos scientific MaxQ 4000 rotary shaker at 25 °C, 30 °C, 35 °C, and 40 °C. Samples of the vancomycin solution were collected at specified time intervals (e.g., 0, 30, 60, 120 mins) to determine the residual concentration of vancomycin remaining in solution.

Adsorption studies using biochar to remove vancomycin were done in batches. For each batch, the adsorbent dosage was 0.1 g/40 ml vancomycin solution. The solution was readjusted to a predetermined pH value using HCl and NaOH. The system was allowed to settle for a predetermined period. Then samples were taken to determine the residual vancomycin concentrations in the solution using a UV-visible spectrophotometer run at 240 nm.

The % removal efficiency was determined, and the adsorption capacity (qe) of vancomycin per gram of biochar was determined using the following formular in equation (1):

$$qe = (C_o - C_e) \times V/m, \tag{1}$$

where qe is the adsorption capacity expressed in mg/g, C_o is the initial concentration of adsorbate vancomycin expressed in mg/L, C_e is the equilibrium concentration of adsorbate, V is the solution volume, and m represents the mass of biochar adsorbent.

3. Result and discussion

3.1. Pyrolysis analysis

The pyrolysis at 400 °C was sufficient to achieve pores in pressed oil palm fruit fibre and also because biochar derived from pressed oil palm fruit fibre, as shown in Figure 3, decreases in percentage yield with an increase in temperature from 350 °C to 650 °C as shown in Figure 4. The bio-oil component decreases with increased pyrolysis temperature while the pyrolysis gas steadily increase with an increase in temperature, similar to the report of Adeoye *et al.* [44].

3.2. XRD analysis

Peaks were observed at 2θ = 19.02 ° and around 21.40 °, which are characteristic crystalline lattices of cellulose, as shown in Figure 5. Adeoye *et al.* [44] described peaks at 2θ equal to 21.77 °, 24.16 °, 27.09 °, and 35.7 °, suggesting diffraction signals of polymorph type I commonly found in native cellulose. The XRD convolution crystallinity index was 47.58%, similar to the palm residue crystallinity index reported in study [45]. The crystallinity of the cellulosic component in the biomass determines its thermal stability, hence indicating the optimal temperature for pyrolysis to produce biochar with quality pores [44]. Pyrolysis of rubber wood sawdust at 500 °C and 700 °C showed cellulose peaks disappearing in XRD spectra since an increase in temperature increases cellulose structure volatilities and thermal degradation starts at 315 °C [46].

3.3. SEM analysis

The scanning electron micrographs in Figure 6 and Figure 7, with magnifications of 80 µm and 50 µm, respectively, showed that there are available pores in the biochar for the adsorption of vancomycin.

Figure 1. Pressed oil palm fruit fibre.

3.4. XRF analysis

The XRF result showed the presence of SiO_2, Al_2O_3, Fe_2O_3, CaO, P_2O_5, TiO_2, MgO, K_2O, SO_3, Mn_2O_5 and Na_2O as presented in Table 1. The SiO_2 has the highest percentage of 84.37%, while Na_2O has the least percentage of 0.04%, as presented in the Table. The presence of iron and manganese in the biochar could positively enhance the adsorption of organic pollutants and improve its stability via processes to include increased surface area and porosity, surface complexation and redox reaction [47]. It has been reported that metal-loaded biochars are potential materials for environmental remediation, such as wastewater treatment and soil pollution clean-up [48].

3.5. BET surface area analysis

The cumulative surface area (SA) of the pyrolysis biochar was 473 m^2/g based on values obtained from methods listed in Table 3. The values of SA obtained in Langmuir method was higher than the BET surface area measurements because the Langmuir model operates under theoretical assumption principles. Biochar obtained via optimized operational parameters such as high temperature or physical activation achieves surface areas above 300 m^2/g. A recent study by Zhao *et al.* [49] reported a range of 150–700 m^2/g for biochar obtained via KOH and steam. The report of Tomczyk *et al.* [50] demonstrated typical biochar BET surface areas to vary between 100–500 m^2/g, which is a close range that aligns with the findings of this present study. The high Langmuir surface area of 1720 m^2/g can be described as an extensive microporosity production through the high pyrolysis temperature activation steps, which makes the biochar appropriate for applications such as antibiotics remediation, CO_2 sequestration and heavy metal elimination. Pore volume is a value that shows the total pore space within the biochar, which reaches 0.109 cm^3/g as shown in Table 2. The cumulative pore volumes for biochar typically range from 0.05 to 0.3 cm^3/g, depending on biomass feedstock and pyrolysis conditions. The pore volume of 0.109 cm^3/g obtained in this study is similar to Inyang *et al.* [51], which reported biochar with cumulative pore volumes extending between 0.1 and 0.3 cm^3/g, which demonstrate potent adsorption capabilities for water pollutants, including heavy metals and organic pollutants. The average pore diameter of the pyrolysis biochar was 3.05 nm, which classifies the biochar as mesoporous according to the IUPAC definition (mesopores: 2–50 nm), which

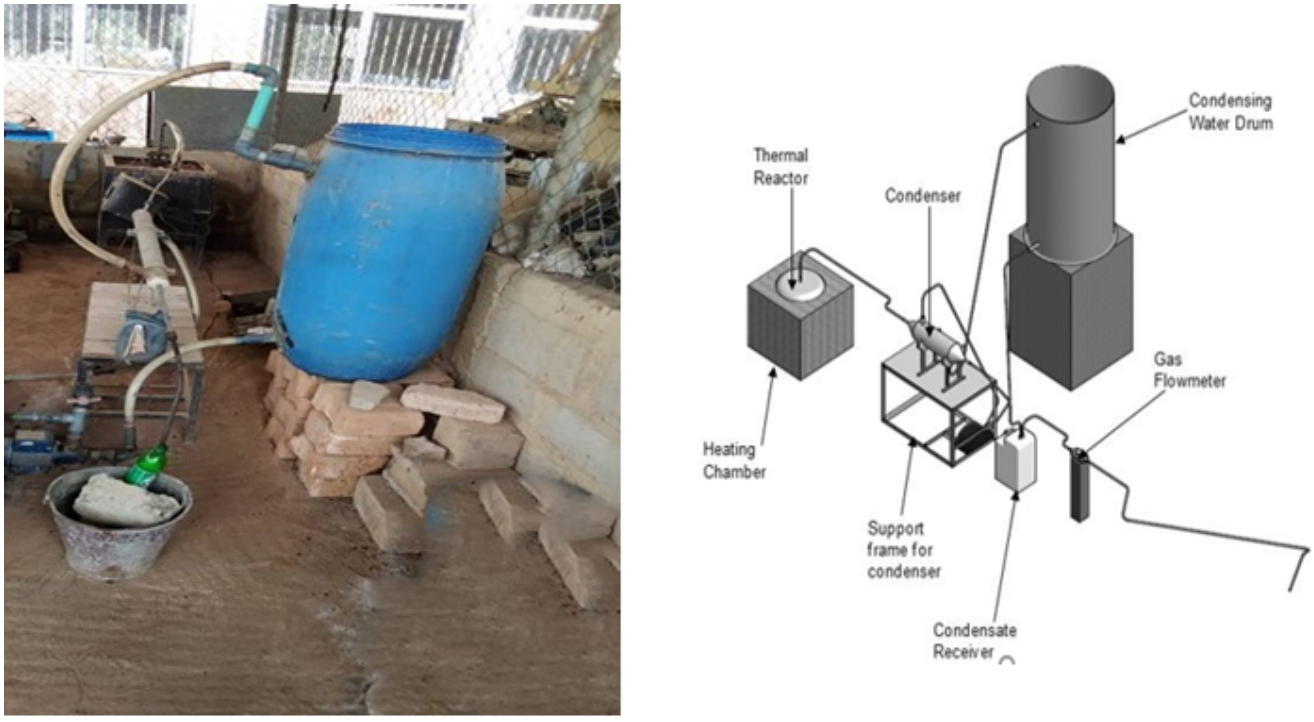

Figure 2. Experimental setup for pyrolysis of pressed oil palm fruit fibre.

Table 1. XRF Analysis of pressed oil palm fruit fibre.

Compounds	SiO_2	Al_2O_3	Fe_2O_3	CaO	MgO	SO_3	K_2O	Na_2O	Mn_2O_5	P_2O_5	TiO_2	LOI
%	84.37	5.14	3.03	2.02	1.10	0.23	1.08	0.04	0.16	1.38	1.20	0.34

LOI- Loss on ignition

Table 2. Surface area of pressed oil palm fruit fibre.

Cumulative surface area	Cumulative pore volumes	Average pore diameter
473.00 m^2/g	0.109 cm^3/g	3.05 nm

Table 3. Methods of surface area of pressed oil palm fruit fibre.

Method	Surface area (m_2/g)
SinglePoint BET	203
MultiPoint BET	328
Langmuir Surface Area	1720
BJH Cumulative Adsorption Surface Area	376
DH Cumulative Adsorption Surface Area	401
t-Method External Surface Area	328
DR Method Micropore Area	356
DFT Cumulative Surface Area	79.2

is similar to the report of Zhao *et al*. [49] with biochars featuring mesoporous diameters in the 2–10 nm range. This range offers excellent potential for applications that need molecular diffusion including organic compound adsorption or catalytic support functions. The mesoporous nature of biochar increases its adsorption rate capacities by promoting molecule reachability into the material. Biochar, with a combined feature of average pore volume alongside its mesoporosity shows the potential to retain water and nutrients effectively when used as a soil remediation [52].

3.6. *Effect of equilibrium time*

The adsorption capacity (qe) of vancomycin per gram of biochar was determined using equation (1). From preliminary experiments as presented in Figure 8, it was observed that adsorption reached a plateau after 60 minutes of contact time, which was used for the adsorption studies.

3.7. *Effect of initial vancomycin concentration*

The data presented in Figure 9 demonstrated the effect of variations in the initial concentration of vancomycin, resulting in a decreasing adsorption percentage as the initial concentration of the antibiotics increased. There was a total removal of vancomycin, 100% at 5 mg/L, while it reduced to almost 29% at a concentration of 25 mg/L, which is similar to trends reported in previous studies [53, 54].

Figure 3. Biochar of pressed oil palm fruit fibre.

3.8. Kinetics of adsorption

Table 3 shows the values of four major kinetic model parameters used in this study. The pseudo-first-order kinetic model presented as equation (2) gave a rate constant K_1 equal to 0.04991 min^{-1} with a high coefficient of correlation of R^2 equal to 0.985, as obtained from the plot in Figure 10. This high R^2 suggests a good fit, which showed that the initial adsorption of vancomycin by the ash follows pseudo first-order behaviour. The low concentration of adsorbate is also responsible for the pseudo first-order kinetics and confirms physisorption is a dominant process as compared to chemisorption, which is similar to Jiao *et al.* [55], who reported a good fit for pseudo first-order kinetics for antibiotics under a specific concentration range at initial rapid adsorption phases. Equation (3) pseudo second-order kinetic model yielded a rate constant K_2 of 0.01795 (g/mg/min) and a strong correlation fit R^2 of 0.943, indicating that the process also experiences chemisorption, as demonstrated by the plot in Figure 11. The R^2 value is lower than that of the pseudo first-order fit, indicating that chemisorption is not the predominant adsorption mechanism. The recent study Wu *et al.* [56] demonstrates that pseudo second-order kinetics in chemisorption cases also accurately fit antibiotic adsorption onto substrates. The Elovich kinetic parameters presented in equation (4) are α (initial adsorption rate) with a value of 1.5232 and β (desorption constant during each experiment) of 0.1312 and a good R^2 value of 0.8513 obtained from Figure 12, which showed that vancomycin adsorption has occurred on heterogenous sites with variation in activation energies, which

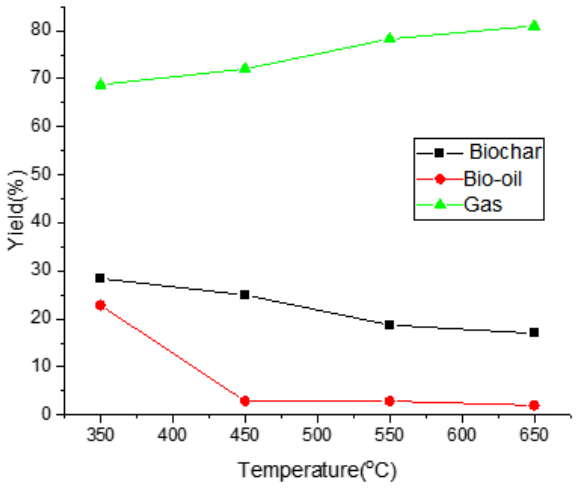

Figure 4. Products distribution in pyrolysis of pressed oil palm fruit fibre at holdtime of 10mins.

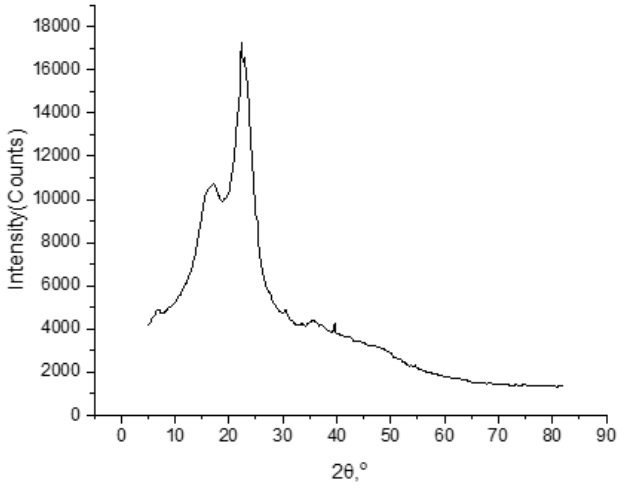

Figure 5. XRD spectrum of pressed oil palm fruit fibre.

helped describe the slowing rate over time during the experiment, which agrees with the findings of Taha *et al.* [57], who observed that antibiotic adsorption on complex adsorbent surfaces usually leads to a decreasing rate as surface saturation occurs. The Avrami kinetic model in equation (5) describes a phase change process as given by its parameters: rate constant k of 0.0348, Avrami exponent (n) of 1.03, and R^2 of 0.976, which implied a multi-step adsorption process for vancomycin obtained from Figure 13. The excellent fit for the model suggests that possible nucleation and growth phases took place on the adsorbent surface due to sequential adsorption. This is similar to the report of Lima *et al.* [58], which gave an indication that the Avrami kinetic model describes perfectly a system where adsorption dynamics shift over time, particularly in heterogeneous systems or multilayer adsorption processes. Pores are formed in the pressed palm fibre via pyrolysis, which is being highlighted by the intraparticle diffusion model on equation (6) to describe their roles in adsorption rate control, particularly in the case of larger molecules (vancomycin) adsorbed in this study with a K_{diff} of 0.1475 and a significant R^2 of 0.651 obtained from Figure 14, which is similar to the study of Zhao *et al.* [59], who identified intraparticle diffusion parameters as significant factors in the adsorption of large biomolecules on porous adsorbents.

The obtained kinetic parameters showed that the adsorption of vancomycin on pyrolyzed pressed palm fibre ash involves both physisorption and chemisorption. The model used offers significant insight into different phases or mechanisms. The complexity for the adsorption of vancomycin is better supported by pseudo-second order and intraparticle diffusion models [54].

$$q_t = q_e\left(1 - e^{k_1 t}\right), \tag{2}$$

where, q_t=Amount adsorbed at time t, q_e=Amount remaining after equilibrium of adsorptionnreaction, K_1=Pseudo-first order rate constant,

$$q_t = \frac{q_e^2 k_2 t}{1 + q_t k_2 t}, \tag{3}$$

where q_t=Amount adsorbed at time t, q_e=Amount remaining after equilibrium of adsorption reaction, K_t=Pseudo-second order rate constant,

$$q_t = \frac{1}{\alpha}\ln(\alpha\beta) + \frac{1}{\alpha}Int, \tag{4}$$

α =Initial adsorption rate β =Desorption constant during each experiment q_t=Amount adsorbed at time t

$$In\left[\ln(\frac{q_e}{q_e - q_t}\right] = nInK + nInt, \tag{5}$$

$$q_t = K_{diff}t^{1/2} + C, \tag{6}$$

3.9. Adsorption isotherm modelling

The mechanisms that controlled the release or mobility of vancomycin in solution to a solid pyrolysis biochar surface at a specific temperature and pH were described by the common adsorption isotherm models Freundlich, Langmuir, Temkin, and Dubinin Radushkevich (D-R) to achieve a clear understanding of adsorbate–adsorbent interaction [60].

The Langmuir equation was described in its linearized form as given in equation (7) [61].

$$\frac{1}{q_e} = \frac{1}{K_L q_{max}}\cdot\frac{1}{C_e} + \frac{1}{q_{max}}, \tag{7}$$

$$R_l = \frac{1}{1 + C_i \times K_l}, \tag{8}$$

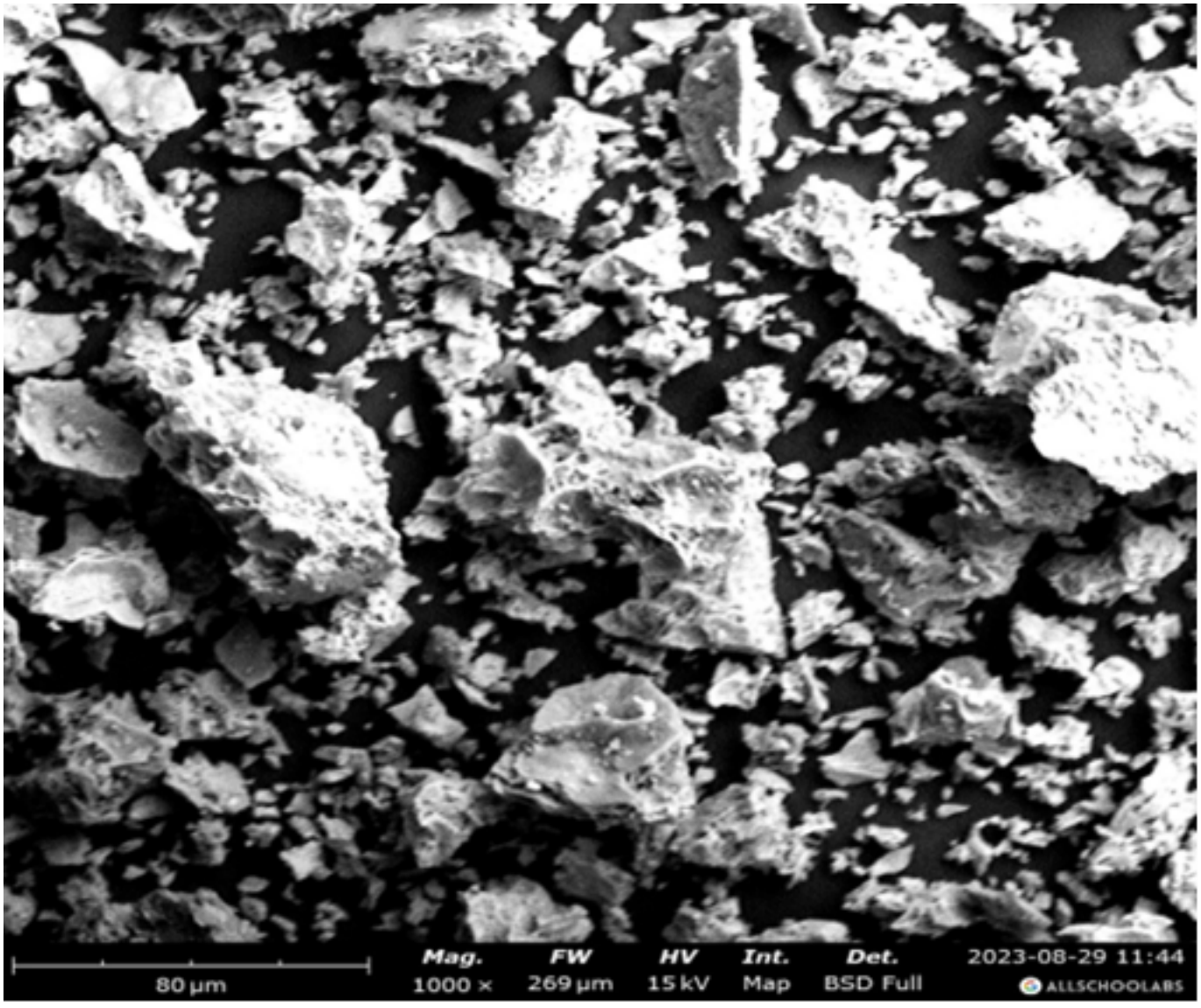

Figure 6. SEM showing biochar pores at 80 µm.

Table 4. Kinetic models parameters.

Pseudo First Order parameters			Pseudo second Order parameters			Elovich kinetic parameters			Avrami kinetic model			Intraparticle diffusion parameters	
K_1 (min^{-1})	qe (mg/g)	R^2	K_2 (g/mgmin)	qe (mg/g)	R^2	α	*B*	R^2	n	K	R^2	K_{diff}	R^2
0.04991	3.48	0.985	0.01795	3.48	0.943	1.5232	0.1312	0.8513	1.03	0.0348	0.976	0.1475	0.651

$$q_{max} = \frac{1}{intercept}, \tag{9}$$

where parameters *qe* is the adsorption capacity at equilibrium (mg/g), qmax is the maximum adsorption capacity (mg/g) obtained from the reciprocal of intercept defined in equation (9), K_L is defined as the Langmuir equilibrium constant, and C_i and Ce represent highest initial concentration and concentration at equilibrium (mg/L) respectively.

A recent study by Bouhamed *et al.* [61] describes the essential features of this model as the separation factor or equilibrium parameter R_L mathematically expressed as shown in equation (8). At $R_L = 0$, the isotherm depicts irreversible adsorption ($R_L = 0$), while the range of favourable adsorption is $0 < R_L < 1$, and the unfavourable adsorption ($R_L > 1$) or linear adsorption

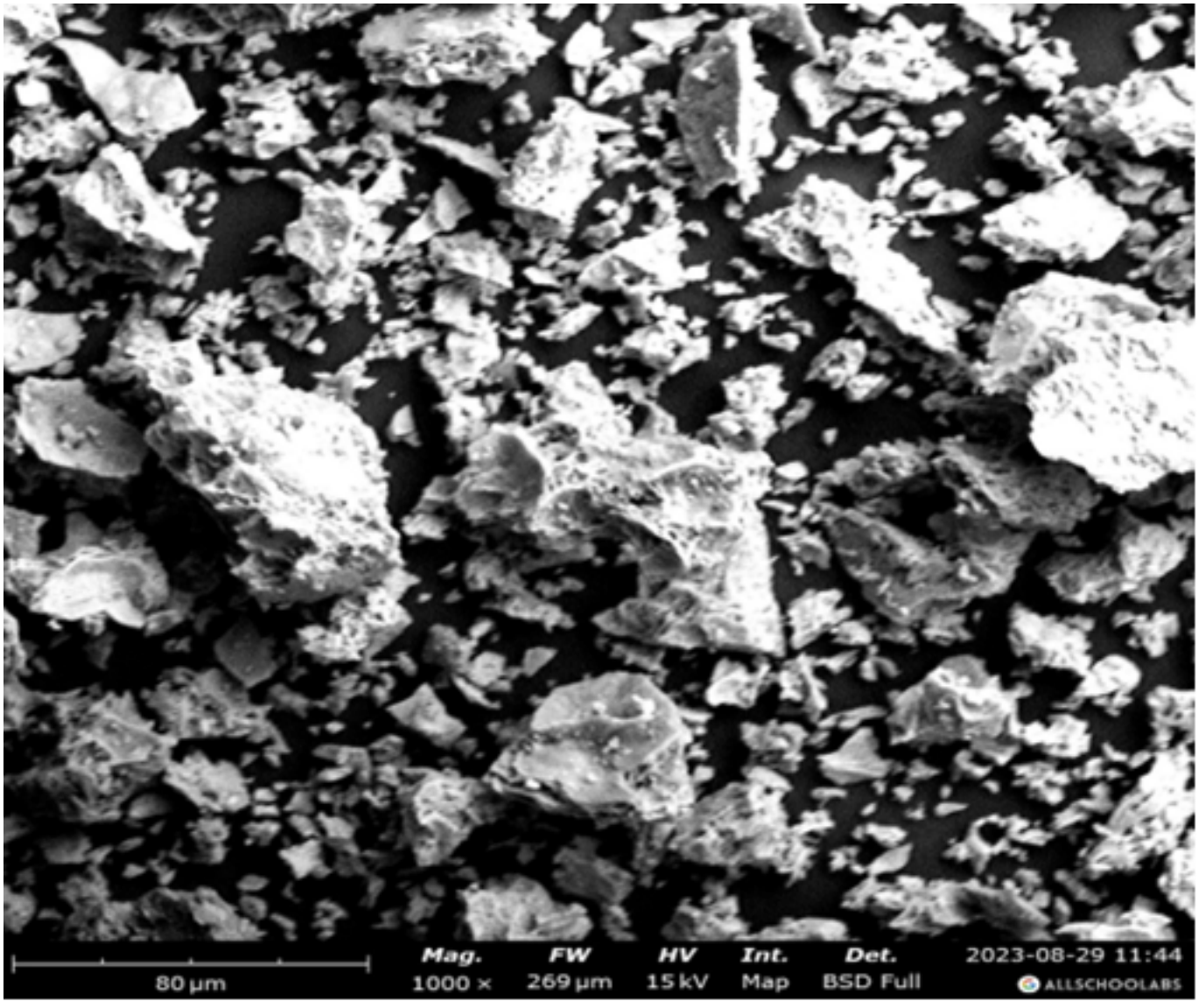

Figure 7. SEM showing biochar pores at 50 µm.

(R_L = 1) is also shown. Adsorption of vancomycin, as shown in Table 4 at different temperatures based on the plot in Figure 15, showed values of R_L at 25 °C, 30 °C, 35 °C, and 40 °C as 0.0498, 0.0464, 0.1667, and 0.1615, which are all less than 1, indicating favourable adsorption.

Equation (10) presented a linearized Freundlich isotherm as given in study [61]:

$$\log q_e = logK_f + \frac{1}{n}\log C_e, \tag{10}$$

$$slope = \frac{1}{n}, \tag{11}$$

$$intercept = \log K_f, \tag{12}$$

where K_F is the Freundlich constant expressed in (mg/g) obtained from equation (12) and the slope equals 1/n, a value that represents the adsorption intensity as defined in equation (11). Table 4 showed the parameters obtained from plots of log (qe) against log(Ce) in Figure 16 at the different temperatures, which showed a straight line was fitted in the data. The adsorption results seem to be well-represented by the Freundlich model, as seen in the correlation constant (R^2), which equals 0.833, 0.828, 0.941, and 0.940 for temperatures of 25 °C, 30 °C, 35 °C, and 40 °C, respectively. The behaviour of the vancomycin during monolayer and multilayer adsorption on the adsorbent is described in this isotherm. The K_f at 25 °C, 30 °C, 35 °C, and 40 °C were 2.020, 2.134, 2.096, and 1.486 (mg/g)*(L/mg)$^{1/n}$, respectively, and n, which characterizes the heterogeneity of the system, was found to be n equals 7.331, 7.953, and 5.190 at these temperatures [62]. All obtained values of n were less than 10 in the Freundlich isotherm, which proved the desirability of VAN adsorption with decreasing affinity, similar to the report of n equals 2.515 when bentonite was used for its adsorption in study [63]. The n value reported is also similar to n values of

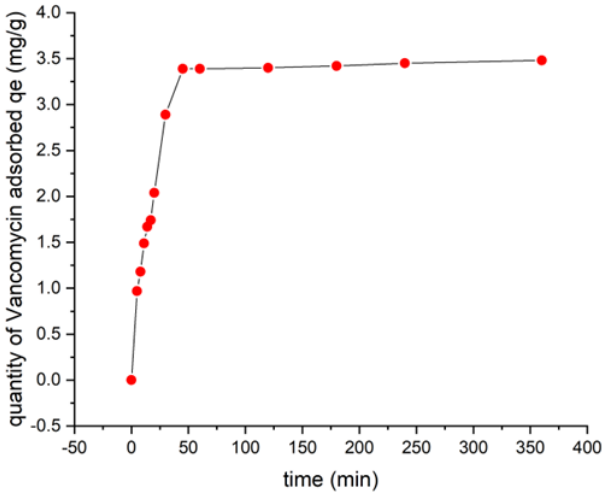

Figure 8. Effect of equilibrium time for vancomycin on biochar. Conditions : pH 6.5, adsorbent dosage 0.1g/40ml, temperature 30°C, concentration: 5.0 mg/L, shaking rate: 100 rpm, shaking time: 60 minutes.

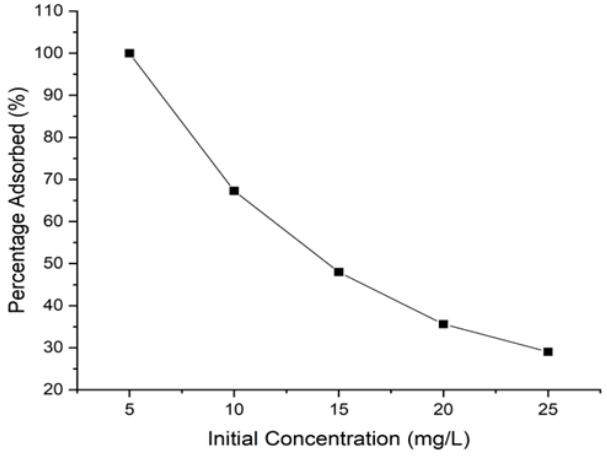

Figure 9. Effect of initial concentration.

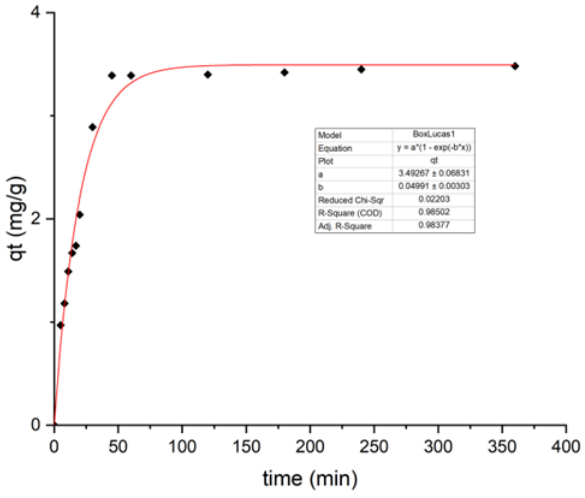

Figure 10. Plot of pseudo-first-order kinetic model.

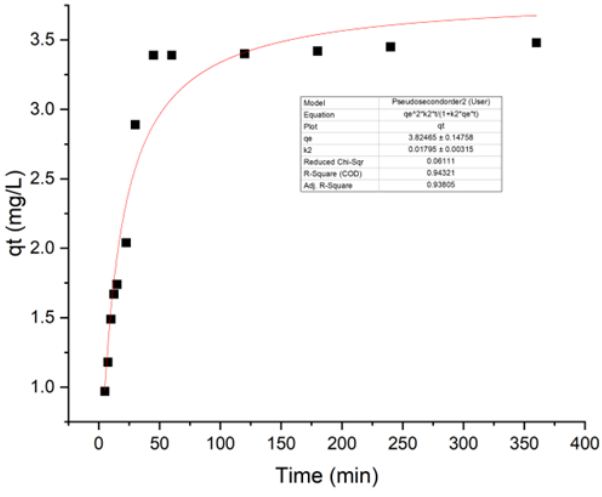

Figure 11. Plot of pseudo-second-order kinetic model.

less than 10 reported in the adsorption of vancomycin in studies [54, 64].

The Temkin isotherm makes assumptions by including parameters that clearly indicate adsorbing species-adsorbent interactions. Adsorbent-adsorbate interactions cause the b_T, or heat of adsorption (J.mol^{-1}), of molecules in the layer to decrease linearly with coverage, and they also govern the adsorption mechanism through a uniform distribution of binding energies, up to a maximum binding energy. The Temkin isotherm model plots at this varied temperature are shown in Figure 17. It gave an acceptable and good fit with correlation constant R^2 of 0.853, 0.845, 0.951, and 0.953 at 25 °C, 30 °C, 35 °C, and 40 °C, respectively, as presented in Table 4. Equation (13) described the isotherm. The obtained b_T, which is equal to the slope from the plots on Figure 17, were 0.320, 0.308, 0.520, and 0.446 (Jmol^{-1}). The b_T values were positive, or the b_T value was less than 1; hence, the adsorption of vancomycin onto the pyrolytic ash is intrinsically endothermic [65]. The Temkin constant K_T defined by equation (14) was 569.938, 1060.221, 54.388, and 105.919 L mg^{-1} at 25 °C, 30 °C, 35 °C, and 40 °C, respectively. The values of the b_T obtained in this study are less than 80 kJ/mol, which also suggests physical adsorption dominance for the adsorption of vancomycin, similar to the report of ampicillin adsorption [66].

$$qe = \frac{RT}{b_T} InK_T + \left(\frac{RT}{b_T}\right) InCe, \tag{13}$$

where: qe = adsorption capacity at equilibrium (mg/g), R = universal gas constant (J.mol^{-1}.K^{-1}), T = temperature (K), b_T = Heat of adsorption (J.mol^{-1}), K_T= Temkim constant (L.mg^{-1}), Ce = Vancomycin final concentration in solution (mg.L^{-1}).

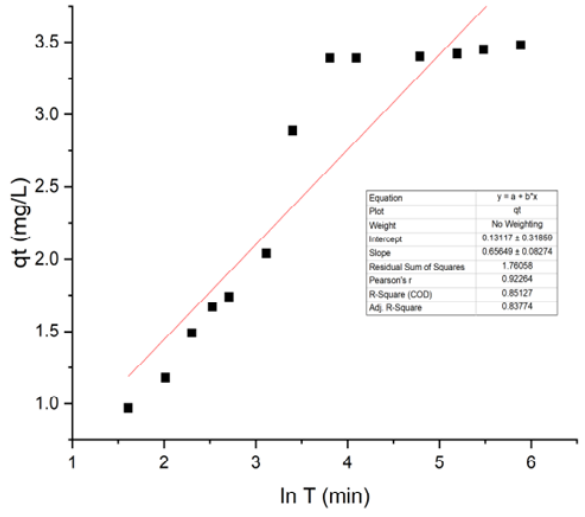

Figure 12. Plot of elovich kinetic model.

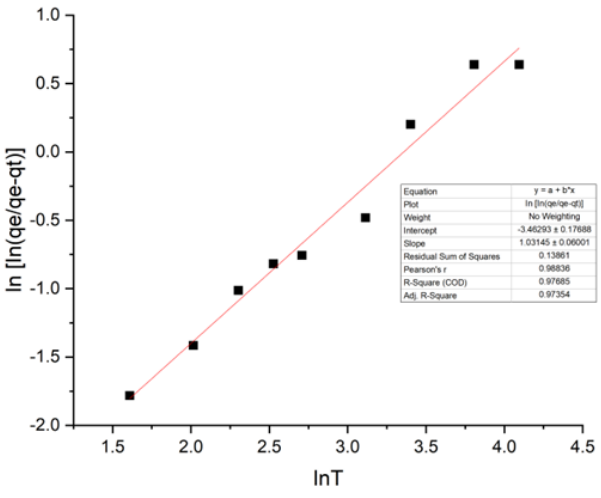

Figure 13. Plot of Avrami kinetic model.

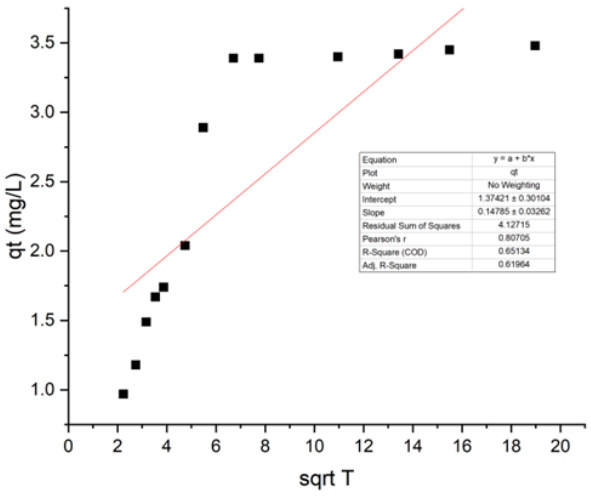

Figure 14. Plot of Intraparticle diffusion.

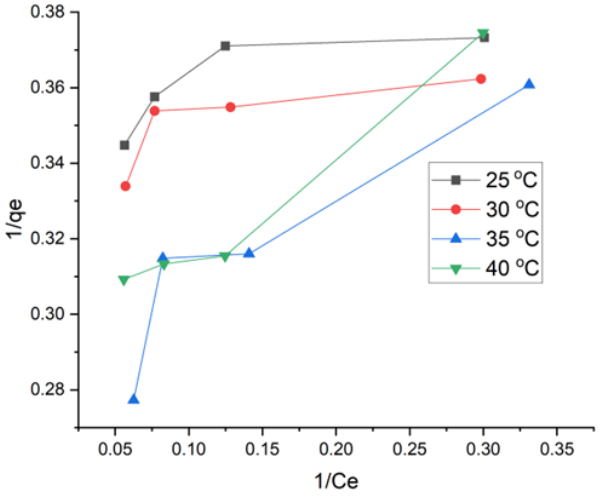

Figure 15. Langmuir isotherm at different temperature.

Temkim constant K_T is defined as shown in equation (14);

$$K_T = e^{\left(\frac{intercept}{b_T}\right)}, \tag{14}$$

Dubinin Radushkevich (D-R) isotherm expressed in equation (15) is given:

$$Inq_e = Inq_m - k\varepsilon^2, \tag{15}$$

$$E = \frac{1}{\sqrt{2K_{D-R}}}, \tag{16}$$

$$\varepsilon = RTIn(1 + \frac{1}{Ce}), \tag{17}$$

where C_e is the equilibrium concentration, qe is the amount adsorbed at equilibrium onto pyrolysed pressed palm fruit fibre (mg/g), qm is adsorption capacity expressed in (mg/g), R is 8.314 J/K/mol, Dubinin Radushkevich isotherm constant is k_{D-R}, T is temperature in kelvin, adsorption potential is expressed in equation (17), and E is the sorption energy defined in equation (16) expressed in (KJ/mol). As seen from the plot in Figure 18, the experimental data in Table 3 fit the model better at higher temperatures (35°C and 40°C), with R^2 values of 0.765 and 0.995, respectively. The E values were 1.552 and 1.448 (KJ/mol), the k_{D-R} isotherm was 4.154 x 10^{-7} and 4.772 x 10^{-7}, and the qm was 3.394 and 3.394 mg/g at 35 °C and 40 °C, respectively. Since the coefficient of correlation of D-R was significantly lower than the other models at 25 °C, 30 °C, and

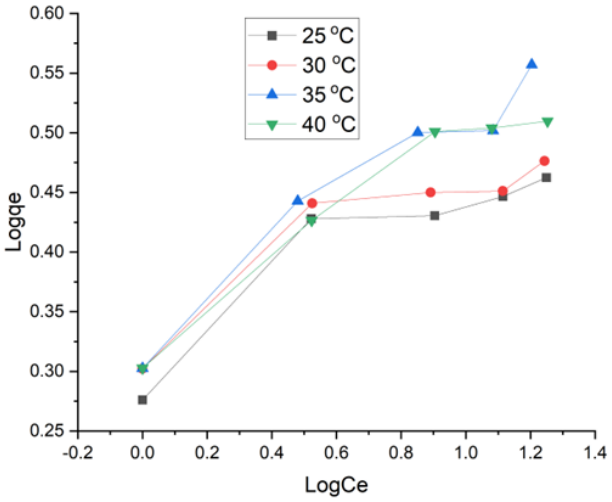

Figure 16. Freundlich isotherm at different temperature.

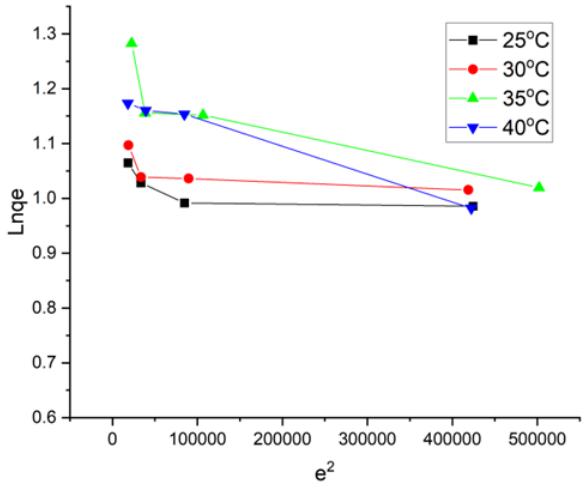

Figure 18. D-R isotherm at different temperature.

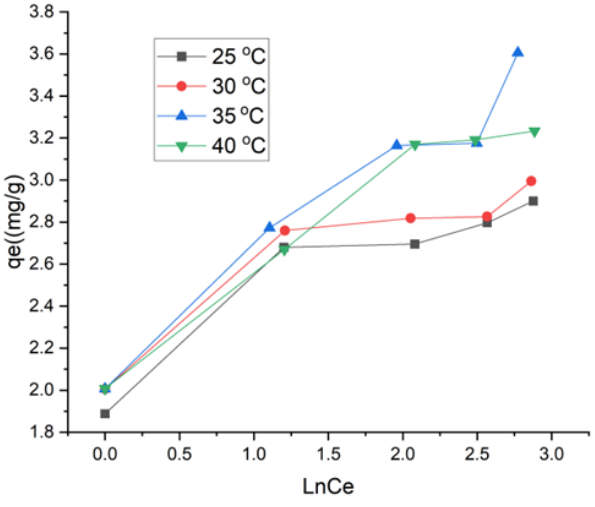

Figure 17. Temkim isotherm at different temperature.

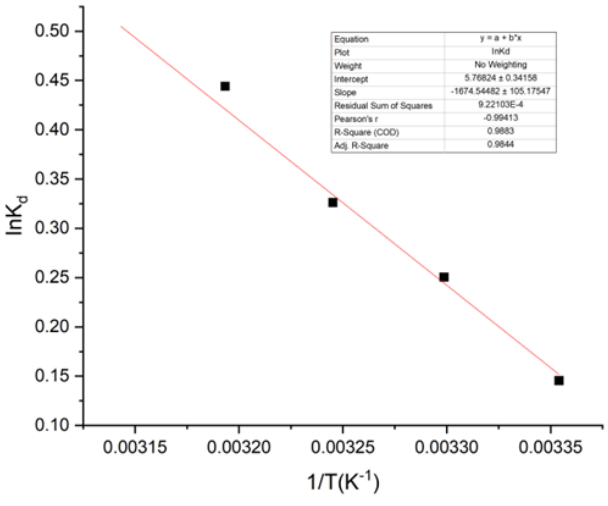

Figure 19. Thermodynamics plots of vancomycin adsorption.

35 °C, it is concluded that the adsorption of vancomycin does not align with a physical process, but at 40 °C, there was alignment with other models that describe physical adsorption took place [59].

3.10. Thermodynamic analysis of adsorption

The determination of the adsorption mechanism to be via physical or chemisorption is not limited to assumptions made from data obtained from isotherm and adsorption kinetic models. The best approach is the combination of analytical techniques and thermodynamic parameters; ΔG, ΔS, ΔH, K_d, and E_a are needed to confirm if the process is a chemical or physical process [67–69]. The thermodynamic parameters presented in Table 5 were obtained using equations (18), (19) and (20).

$$K_d = \frac{q_e}{C_e}, \tag{18}$$

where K_d is the adsorption equilibrium constant, Ce is the equilibrium concentration, qe is the equilibrium adsorption constant

$$InK_d = \frac{\Delta S}{R} - \frac{\Delta H}{RT}, \tag{19}$$

$$\Delta G = \Delta H - T\Delta S, \tag{20}$$

where ΔG is the free energy, ΔH is the change of enthalpy, and ΔS is the change of entropy.

The analysis result was used to explain physical adsorption, which is the main mechanism responsible for the adsorption of vancomycin, described as an exothermic process as presented by the change in enthalpy values (ΔH) in Table 5, and the resulting standard Gibbs energy (ΔG°) values were determined. Negative ΔG^o values ranging from −28.94 to −13.92 kJ/mol demonstrate that the adsorption of vancomycin is favourable

Table 5. Data of isotherm models.

	Temkim isotherm parameters			D-R isotherm parameters			
T (^{o}C)	K_T(Lmg^{-1})	B_T(Jmol^{-1})	R^2	E(KJ/mol)	k	q_mD-R	R^2
					D−R isotherm constant		
25	569.938	0.320	0.853	0.002	0.400	2.818	0.475
30	1060.221	0.308	0.845	0.001	0.464	2.899	0.464
35	54.388	0.520	0.951	1.552	4.154x 10^{-7}	3.394	0.765
40	105.919	0.446	0.953	1.448	4.772x 10^{-7}	3.269	0.995

	Langmuir isotherm parameters				Freundlich isotherm parameters			
T (°C)	q_{max}(mg/g)	K_L (L/mg)	R_L	R^2	K_f	n	1/n	R^2
25	2.866	3.816	0.0498	0.592	2.020	7.331	0.136	0.833
30	2.944	4.110	0.0464	0.557	2.134	7.953	0.126	0.828
35	3.902	1.000	0.1667	0.847	2.096	5.190	0.193	0.941
40	3.461	1.039	0.1615	0.967	1.486	5.828	0.172	0.940

Table 6. Thermokinetics parameters.

Temp. (°C)	K_d	ΔS° (J/mol.K)	ΔH° (KJ/mol)	ΔG° (KJ/mol)
25	1.157			-28.22
30	1.285	0.048	-13.92	-13.92
35	1.385			-28.70
40	1.559			-28.94

and spontaneous over the experimented temperatures of 25 °C, 30 °C, 35 °C, and 40 °C, i.e., ($\Delta G^\circ > -28.94$, $\Delta S > 0$). The favourable and spontaneous cases from the thermodynamic parameters confirm the conclusions based on the values of n from the Freundlich isotherm and R_L from the Langmuir isotherm. An antibiotic adsorption study by Al-Mousavi et al. [66] reported standard free energy in the range of −8.69 to −2.94 kJ/mol, which is also in the range of −28.94 to −13.92 kJ/mol obtained in this study; hence it can be concluded that the adsorption of vancomycin has a physical process. From the obtained negative enthalpy value ΔH of -13.92 kJ/mol, it can be concluded that vancomycin adsorption was exothermic and spontaneous. The ΔH values of -13.92 kJ/mol also confirm the physical mechanism of adsorption, similar to the report of studies [70, 71]. The K_d increases steadily from 1.157 to 1.559 with an increase in temperature, as shown in Figure 18. The thermodynamic data clearly indicates the dominant physical nature of the vancomycin adsorption process since R^2 for pseudo first and second order is higher than the value of R^2 of 0.8513 obtained from the Elovich model, which assumes chemical adsorption.

4. Conclusion

This study examined vancomycin adsorption on a pyrolysis biochar of pressed palm fruit fibre, varying the initial concentration, pH, and amount of adsorbent material. The results indicated that a pH of 6.5 was optimal. As the amount of adsorbent increases, the adsorption percentage increases, and vice versa as the starting concentration increases. The coefficient of R^2 of isotherm models including Temkim, D-R, Langmuir, and Freundlich, respectively, was close to 1 at 40°C. The ΔG° and ΔS values demonstrate that the adsorption of vancomycin is favourable and spontaneous. The adsorption process was mainly via a physical process, spontaneous and exothermic, since ΔH° is negative.

The physicochemical properties of biochar that were obtained are equivalent to those of activated biochar, characterized by an exceptional surface area, average cumulative pore volume, and mesoporous diameter, making it appropriate for organic contaminant adsorption, soil applications, and catalytic processes.

The study recommends pyrolysis biochar of pressed palm oil fruit fibre as a sustainable, cheap, and eco-friendly material for remediating vancomycin from water. Further studies should investigate using this biochar to adsorb other organic contaminants.

Data Availability

We do not have any research data outside the submitted manuscript file.

References

[1] X. Chang, M. T. Meyer, X. Liu, Q. Zhao, H. Chen, J. Chen, Z. Qiu, L. Yang, J. Cao & W. Shu, "Determination of antibiotics in sewage from hospitals, nursery and slaughter house, wastewater treatment plant and source water in Chongqing region of Three Gorge Reservoir in China", Environmental Pollution **158** (2010) 1444. https://doi.org/10.1016/j.envpol.2009.12.034.

[2] N. Alavi, A. A. Babaei, M. Shirmardi, A. Naimabadi & G. Goudarzi, "Assessment of oxytetracycline and tetracycline antibiotics in manure samples in different cities of Khuzestan Province, Iran", Environmental Science and Pollution Research **22** (2015) 17948. https://doi.org/10.1007/s11356-015-5002-9.

[3] M. I. Hutchings, A. W. Truman & B. Wilkinson, "Antibiotics: past, present and future", Current Opinion in Microbiology **51** (2019) 72. https://doi.org/10.1016/j.mib.2019.10.008.

[4] L. Serwecińska, "Antimicrobials and antibiotic-resistant bacteria: a risk to the environment and to public health", Water **12** (2020) 3313. https://doi.org/10.3390/w12123313.

[5] A. Saravanan, P. S. Kumar, S. Jeevanantham, S. Karishma, B. Tajsabreen, P. Yaashikaa & B. Reshma, "Effective water/wastewater treatment methodologies for toxic pollutants removal: Processes and applications towards sustainable development", Chemosphere **280** (2021) 130595. https://doi.org/10.1016/j.chemosphere.2021.130595.

[6] T. C. M. Vinh Do, D. Q. Nguyen, T. D. Nguyen & P. H. Le, "Development and Validation of a LC-MS/MS Method for Determination of Multi-Class Antibiotic Residues in Aquaculture and River Waters, and Photocatalytic Degradation of Antibiotics by TiO_2 Nanomaterials", Catalysts **10** (2020) 356. https://doi.org/10.3390/catal10030356.

[7] C. Monahan, R. Nag, D. Morris & E. Cummins, "Antibiotic residues in the aquatic environment – current perspective and risk considerations", Journal of Environmental Science and Health Part A **56** (2021) 733. https://doi.org/10.1080/10934529.2021.1923311.

[8] R. Selvarajan, C. Obize, T. Sibanda, A. L. K. Abia & H. Long, "Evolution and Emergence of Antibiotic Resistance in Given Ecosystems: Possible Strategies for Addressing the Challenge of Antibiotic Resistance", Antibiotics **12** (2022) 28. https://doi.org/10.3390/antibiotics12010028.

[9] V. M. Pathak, V. K. Verma, B. S. Rawat, B. Kaur, N. Babu, A. Sharma, S. Dewali, M. Yadav, R. Kumari, S. Singh, A. Mohapatra, V. Pandey, N. Rana & J. M. Cunill, "Current status of pesticide effects on environment, human health and it's eco-friendly management as bioremediation: A comprehensive review", Frontiers in Microbiology **13** (2022) 962619. https://doi.org/10.3389/fmicb.2022.962619.

[10] S. Khan, Mu. Naushad, M. Govarthanan, J. Iqbal & S. M. Alfadul, "Emerging contaminants of high concern for the environment: Current trends and future research", Environmental Research **207** (2021) 112609. https://doi.org/10.1016/j.envres.2021.112609.

[11] R. Changotra, A. Chalotra & H. Rajput, "Antibiotics and resistance in environment", in *Emerging Modalities in Mitigation of Antimicrobial Resistance*, Akhtar, N., Singh, K. S., Prerna, Goyal, D. (eds), Springer, Cham. Switzerland, AG, 2022, pp. 23–46. http://dx.doi.org/10.1007/978-3-030-84126-3_2.

[12] D. S. Read, H. S. Gweon, M. J. Bowes, M. F. Anjum, D. W. Crook, K. K. Chau, L. P. Shaw, A. Hubbard, M. AbuOun, H. J. Tipper, S. J. Hoosdally, M. J. Bailey, A. S. Walker & N. Stoesser, "Dissemination and Persistence of Antimicrobial Resistance (AMR) along the wastewater-river continuum", Water Research **264** (2024) 122204. https://doi.org/10.1016/j.watres.2024.122204.

[13] A. Singh, S. Saluja, "Microbial degradation of antibiotics from effluents", in *Recent Advances in Microbial Degradation*, Environmental and Microbial Biotechnology, Springer, Singapore, 2021, pp. 389–404. https://link.springer.com/chapter/10.1007/978-981-16-0518-5_15.

[14] A. Alengebawy, S. T. Abdelkhalek, S. R. Qureshi & M.-Q. Wang, "Heavy metals and pesticides toxicity in agricultural soil and plants: ecological risks and human health implications", Toxics **9** (2021) 42. https://doi.org/10.3390/toxics9030042.

[15] E. S. Okeke, K. I. Chukwudozie, R. Nyaruaba, R. E. Ita, A. Oladipo, O. Ejeromedoghene, E. O. Atakpa, C. V. Agu & C. O. Okoye, "Antibiotic resistance in aquaculture and aquatic organisms: a review of current nanotechnology applications for sustainable management", Environmental Science and Pollution Research **29** (2022) 69241. https://doi.org/10.1007/s11356-022-22319-y.

[16] S. Squadrone, "Water environments: metal-tolerant and antibiotic-resistant bacteria", Environmental Monitoring and Assessment **192** (2020) 238. https://doi.org/10.1007/s10661-020-8191-8.

[17] E. Felis, J. Kalka, A. Sochacki, K. Kowalska, S. Bajkacz, M. Harnisz & E. Korzeniewska, "Antimicrobial pharmaceuticals in the aquatic environment - occurrence and environmental implications", European Journal of Pharmacology **866** (2019) 172813. https://doi.org/10.1016/j.ejphar.2019.172813.

[18] M. M. Jacob, M. Ponnuchamy, A. Kapoor, D. B. Pal & P. Sivaraman, "Biochar innovations for adsorption of water contaminants in water treatment", in *Clean Energy Production Technologies*, springer, Singapore, 2024, 183–201. https://doi.org/10.1007/978-981-97-0847-5_9.

[19] B. Chen, D. Zhou & L. Zhu, "Transitional adsorption and partition of nonpolar and polar aromatic contaminants by biochars of pine needles with different pyrolytic temperatures", Environmental Science & Technology **42** (2008) 5137. https://doi.org/10.1021/es8002684.

[20] L. A. Abudu, H. R. Sadabad, T. Oluseyi, D. Adeyemi, L. A. Adams & H. M. Coleman, *Removal of vancomycin from water by adsorption using waste materials*, Masters thesis, Ulster University, Ulster, 2023. https://pure.ulster.ac.uk/en/publications/removal-of-vancomycin-from-water-by-adsorption-using-waste-materi.

[21] J. Hollis. "The development and characterization of a vancomycin nanostructured lipid carrier and evaluation of their antimicrobial properties on Staphylococcus aureus", Masters thesis, University of Central Lancashire, Preston, Lancashire, 2024. http://doi.org/10.17030/uclan.thesis.00052737.

[22] M. Barathan, S.-L. Ng, Y. Lokanathan, M. H. Ng & J. X. Law, "Unseen weapons: bacterial extracellular vesicles and the spread of antibiotic resistance in aquatic environments", International Journal of Molecular Sciences **25** (2024) 3080. https://doi.org/10.3390/ijms25063080.

[23] X. Q. Cheng, C. Zhang, Z. X. Wang & L. Shao, "Tailoring nanofiltration membrane performance for highly-efficient antibiotics removal by mussel-inspired modification", Journal of Membrane Science **499** (2015) 326. https://doi.org/10.1016/j.memsci.2015.10.060.

[24] L. Xu, J. Dai, J. Pan, X. Li, P. Huo, Y. Yan, X. Zou & R. Zhang, "Performance of rattle-type magnetic mesoporous silica spheres in the adsorption of single and binary antibiotics", Chemical Engineering Journal **174** (2011) 221. https://doi.org/10.1016/j.cej.2011.09.003.

[25] Z. Bai, Q. Yang & J. Wang, "Catalytic ozonation of sulfamethazine antibiotics using $Ce_{0.1}$ $Fe_{0.9}OOH$: Catalyst preparation and performance", Chemosphere **161** (2016) 174. https://doi.org/10.1016/j.chemosphere.2016.07.012.

[26] N. F. Moreira, J. M. Sousa, G. Macedo, A. R. Ribeiro, L. Barreiros, M. Pedrosa, J. L. Faria, M. F. R. Pereira, S. Castro-Silva, M. A. Segundo, C. M. Manaia, O. C. Nunes & A. M. Silva, "Photocatalytic ozonation of urban wastewater and surface water using immobilized TiO_2 with LEDs: Micropollutants, antibiotic resistance genes and estrogenic activity", Water Research **94** (2016) 10. https://doi.org/10.1016/j.watres.2016.02.003.

[27] H. Niu, N. Dizhang, Z. Meng & Y. Cai, "Fast defluorination and removal of norfloxacin by alginate/Fe@Fe_3O_4 core/shell structured nanoparticles", Journal of Hazardous Materials **227** (2012) 195. https://doi.org/10.1016/j.jhazmat.2012.05.036.

[28] J. A. De Lima Perini, M. Perez-Moya & R. F. P. Nogueira, "Photo-Fenton degradation kinetics of low ciprofloxacin concentration using different iron sources and pH", Journal of Photochemistry and Photobiology a Chemistry **259** (2013) 53. https://doi.org/10.1016/j.jphotochem.2013.03.002.

[29] L. Demarchis, M. Minella, R. Nisticò, V. Maurino, C. Minero & D. Vione, "Photo–Fenton reaction in the presence of morphologically controlled hematite as iron source", Journal of Photochemistry and Photobiology a Chemistry **307** (2015) 99. https://doi.org/10.1016/j.jphotochem.2015.04.009.

[30] M. S. Díaz-Cruz & D. Barceló, "LC–MS2 trace analysis of antimicrobials in water, sediment and soil", TrAC Trends in Analytical Chemistry **24** (2005) 645. https://doi.org/10.1016/j.trac.2005.05.005.

[31] A. Göbel, A. Thomsen, C. S. McArdell, A. Joss & W. Giger, "Occurrence and sorption behavior of sulfonamides, macrolides, and trimethoprim in activated sludge treatment", Environmental Science & Technology **39** (2005) 3981. https://doi.org/10.1021/es048550a.

[32] K. Li, A. Yediler, M. Yang, S. Schulte-Hostede & M. H. Wong, "Ozonation of oxytetracycline and toxicological assessment of its oxidation by-products", Chemosphere **72** (2008) 473. https://doi.org/10.1016/j.chemosphere.2008.02.008.

[33] A. G. Trovo, R. F. P. Nogueira, A. Agüera, A.R. Fernandez-Alba & S. Malato, "Degradation of the antibiotic amoxicillin by photo Fenton process–chemical and toxicological assessment", Water Resource **45** (2011) 1394. https://doi.org/10.1016/j.watres.2010.10.029.

[34] A. Gulkowska, H. Leung, M. So, S. Taniyasu, N. Yamashita, L. W. Yeung, B. J. Richardson, A. Lei, J. Giesy & P. K. Lam, "Removal of antibiotics from wastewater by sewage treatment facilities in Hong Kong and Shenzhen, China", Water Research **42** (2007) 395. https://doi.org/10.1016/j.watres.2007.07.031.

[35] S. Lenore, E. Arnold & D. Andrew, "Standard methods for the examination of water and wastewater", American Public Health Association, Washington, DC, 1998, pp. 212–234. https://search.worldcat.org/title/Standard-methods-for-the-examination-of-water-and-wastewater/oclc/40733179.

[36] A. A. Babaei, Z. Alaee, E. Ahmadpour & A. Ramazanpour-Esfahani, "Kinetic modeling of methylene blue adsorption onto acid-activated spent

tea: A comparison between linear and non-linear regression analysis", Journal of Advances in Environmental Health Research **2** (2014) 197. https://doi.org/10.22102/jaehr.2014.40170.

[37] M. S. Legnoverde, S. Simonetti & E. I. Basaldella, "Influence of pH on cephalexin adsorption onto SBA-15 mesoporous silica: Theoretical and experimental study", Applied Surface Science **300** (2014) 37. https://doi.org/10.1016/j.apsusc.2014.01.198.

[38] H. R. Pouretedal & N. Sadegh, "Effective removal of Amoxicillin, Cephalexin, Tetracycline and Penicillin G from aqueous solutions using activated carbon nanoparticles prepared from vine wood", Journal of Water Process Engineering **1** (2014) 64. https://doi.org/10.1016/j.jwpe.2014.03.006.

[39] Y. Jia, Y. Ou, S. K. Khanal, L. Sun, W.-S. Shu & H. Lu, "Biochar-based strategies for antibiotics removal: mechanisms, factors, and application", ACS ES&T Engineering **4** (2024) 1256. https://doi.org/10.1021/acsestengg.3c00605.

[40] A. K. Patel, R. Katiyar, C. Chen, R. R. Singhania, M. K. Awasthi, S. Bhatia, T. Bhaskar & C. Dong, "Antibiotic bioremediation by new generation biochar: Recent updates", Bioresource Technology **358** (2022) 127384. https://doi.org/10.1016/j.biortech.2022.127384.

[41] R. Katiyar, C. Chen, R. R. Singhania, M. Tsai, G. D. Saratale, A. Pandey, C. Dong & A. K. Patel, "Efficient remediation of antibiotic pollutants from the environment by innovative biochar: current updates and prospects", Bioengineered **13** (2022) 14730. https://doi.org/10.1080/21655979.2022.2108564.

[42] M. Pan, "Biochar adsorption of antibiotics and its implications to remediation of contaminated soil", Water Air & Soil Pollution **231** (2020) 221. https://doi.org/10.1007/s11270-020-04551-9.

[43] A. O Adeoye, R. O. Quadri & O. S. Lawal, "Fixed-bed pyrolysis and thermal analyses of pressed oil palm fruit fiber as a potential alternative energy", FUOYE Journal of Innovation Science and Technology **2** (2022) 1. https://jist.fuoye.edu.ng/index.php/jist/article/view/46.

[44] A. O. Adeoye, R. O. Quadri & O. S. Lawal, "Assessment of biofuel potential of tenera palm kernel shell via fixed bed pyrolysis and thermal characterization", Results in Surfaces and Interfaces **9** (2022) 100091. https://doi.org/10.1016/j.rsurfi.2022.100091.

[45] E. C. Okoroigwe, C.M. Saffron & P. D. Kamdem, "Characterization of palm kernel shell for materials reinforcement and water treatment", Journal of Chemical Engineering and Materials Science **5** (2014) 1. http://dx.doi.org/10.5897/JCEMS2014.0172.

[46] A. Shaaban, S.-M. Se, N. M. M. Mitan & M. F. Dimin, "Characterization of Biochar Derived from Rubber Wood Sawdust through Slow Pyrolysis on Surface Porosities and Functional Groups", Procedia Engineering **68** (2013) 365. https://doi.org/10.1016/j.proeng.2013.12.193.

[47] Y. Dong, J. E. Z. Liang, J. Song, C. Liu, Z. Ding, W. Wang & W. Zhang, "Preparation of biochar/iron mineral composites and their adsorption of methyl orange", RSC Advances **14** (2024) 33977. https://doi.org/10.1039/d4ra05529b.

[48] M. a. A. Masud, W. S. Shin, A. Sarker, A. Septian, K. Das, K., D. M. Deepo, M. A. Iqbal, A. R. M. T. Islam & G. Malafaia, "A critical review of sustainable application of biochar for green remediation: Research uncertainty and future directions", The Science of the Total Environment **904** (2023) 166813. https://doi.org/10.1016/j.scitotenv.2023.166813.

[49] L. Zhao, W. Zheng, O. Mašek, X. Chen, B. Gu, B. K. Sharma & X. Cao, "Roles of phosphoric acid in biochar formation: synchronously improving carbon retention and sorption capacity", Journal of Environmental Quality **46** (2017) 393. https://doi.org/10.2134/jeq2016.09.0344.

[50] A. Tomczyk, Z. Sokołowska & P. Boguta, "Biochar physicochemical properties: Pyrolysis temperature and feedstock kind effects", Reviews in Environmental Science and BioTechnology **19** (2020) 191. https://doi.org/10.1007/s11157-020-09523-3.

[51] M. I. Inyang, B. Gao, Y. Yao, Y. Xue, A. Zimmerman, A. Mosa, P. Pullammanappallil, Y. S. Ok & X. Cao, " A review of biochar as a low-cost adsorbent for aqueous heavy metal removal", Critical Reviews in Environmental Science and Technology **46** (2016) 406. https://doi.org/10.1080/10643389.2015.1096880.

[52] J. Lehmann & S. Joseph, "Biochar for environmental management: science, technology, and implementation", Routledge, 2015. https://www.routledge.com/Biochar-for-Environmental-Management-Science-Technology.

[53] M. G. Ghozikali, A. Mohammadpour & R. Dehghanzadeh, "Utilization of Activated Carbon Catalyzed Ozonation (ACCO) for removal of ciprofloxacin and vancomycin from hospital wastewater", Iranian Journal of Public Health **52** (2023) 1522. https://doi.org/10.18502/ijph.v52i7.13255.

[54] F. Gashtasbi, R. J. Yengejeh & A. A. Babaei, "Adsorption of vancomycin antibiotic from aqueous solution using an activated carbon impregnated magnetite composite", Desalination and Water Treatment **88** (2017) 286. https://doi.org/10.5004/dwt.2017.21455.

[55] P. Jiao, X. Zhang, Y. Wei & Y. Meng, "Adsorption equilibria, kinetics, and column dynamics of l-tryptophan on mixed-mode resin HD-1", ACS Omega **7** (2022) 9614. https://doi.org/10.1021/acsomega.1c06960.

[56] J. Wu, H. Wang, H. Shen, C. Shen, Y. Zhu, J. Wu & H. Ran, "Experimental and Kinetic Analysis of H_2O on Hg^0 Removal by Sorbent Traps in Oxy-combustion Atmosphere", Industrial & Engineering Chemistry Research **60** (2021) 12200. https://doi.org/10.1021/acs.iecr.1c01636.

[57] M. Taha, A. Elsayed, M. Abbas, H. Fakhry & E. M. Ali, "Bio-sorption of Methyl blue from Synthetic wastewater onto copper\zinc oxides Bimetallic Nanoparticles Synthesized by Fusarium oxysporum: Equilibrium isotherms, Kinetic models, Process optimization, and Antibacterial activity", Egyptian Journal of Chemistry **67** (2023) 513. https://doi.org/10.21608/ejchem.2023.213597.8029.

[58] E. C. Lima, A. R. Cestari & M. A. Adebayo, "Comments on the paper: a critical review of the applicability of Avrami fractional kinetic equation in adsorption-based water treatment studies", Desalination and Water Treatment **57** (2015) 19566. https://doi.org/10.1080/19443994.2015.1095129.

[59] W. Zhao, L. Yang, W. Han, C. Gu, Z. Xu, X. Lv & H. Zhang, "Application and evaluation of a modified intraparticle diffusion model for mono-/multiadsorption of chlorobenzene pollutants on biochar", Journal of Soils and Sediments **24** (2024) 3626. https://doi.org/10.1007/s11368-024-03910-x.

[60] D. AO, "Langmuir, Freundlich, Temkin and Dubinin–Radushkevich Isotherms Studies of Equilibrium Sorption of Zn^{2+} Unto Phosphoric Acid Modified Rice Husk", IOSR Journal of Applied Chemistry **3** (2012) 38. https://doi.org/10.9790/5736-0313845.

[61] F. Bouhamed, Z. Elouear & J. Bouzid, "Adsorptive removal of copper (II) from aqueous solutions on activated carbon prepared from Tunisian date stones: Equilibrium, kinetics and thermodynamics", Journal of the Taiwan Institute of Chemical Engineers **43** (2012) 741. https://doi.org/10.1016/j.jtice.2012.02.011.

[62] Z. F. Akl, "Theoretical and experimental studies on uranium(vi) adsorption using phosphine oxide-coated magnetic nanoadsorbent", RSC Advances **11** (2021) 39233. https://doi.org/10.1039/d1ra04515f.

[63] A. Ebrahimi, M. Ehteshami & B. Dahrazma, "Biosorption of Cd (II) from aqueous solutions using Crataegus oxyacantha stone and Punica granatum seed", Desalination and Water Treatment **57** (2015) 9354. https://doi.org/10.1080/19443994.2015.1029005.

[64] B. Delmond, S. Tretsiakova-McNally, B. Solan, R. McDermott & A. Audoin, "A Sustainable Method to Reduce Vancomycin Concentrations in Water Using Timber Waste", Water Air & Soil Pollution **234** (2023) 9. https://doi.org/10.1007/s11270-023-06070-9.

[65] Z. Huang, Y. Li, W. Chen, J. Shi, N. Zhang, X. Wang, Z. Li, L. Gao & Y. Zhang, "Modified bentonite adsorption of organic pollutants of dye wastewater", Materials Chemistry and Physics **202** (2017) 266. https://doi.org/10.1016/j.matchemphys.2017.09.028.

[66] T. J. Al-Musawi, N. Mengelizadeh, M. Taghavi, S. Mohebi & D. Balarak, "Activated carbon derived from Azolla filiculoides fern: a high-adsorption-capacity adsorbent for residual ampicillin in pharmaceutical wastewater", Biomass Conversion and Biorefinery **13** (2021) 12179. https://doi.org/10.1007/s13399-021-01962-4.

[67] H. N. Tran, S.-J. You & H.-P. Chao, "Thermodynamic parameters of cadmium adsorption onto orange peel calculated from various methods: A comparison study", Journal of Environmental Chemical Engineering **4** (2016) 2671. https://doi.org/10.1016/j.jece.2016.05.009.

[68] É. C. Lima, M. A. Adebayo, F. M. Machado, "Machado Kinetic and Equilibrium Models of Adsorption", In: *Carbon Nanomaterials as Adsorbents for Environmental and Biological Applications*, C. Bergmann, F. Machado, (eds), Carbon Nanostructures, Springer, Cham. 2015, pp. 33–69. https://doi.org/10.1007/978-3-319-18875-1_3.

[69] O. Safranin, "dye removal using Senna fistula activated biomass: Kinetic, equilibrium and thermodynamic studies", Journal of the Nigerian Society of Physical Sciences **5** (2022) 951. https://doi.org/10.46481/jnsps.2023.

951.

[70] E. Kazrafshan, M. Sobhanikia & F. K. Mostafapour, "Chromium biosorption from aqueous environments by mucilaginous seeds of Cydonia oblonga: Thermodynamic, equilibrium and kinetic studies", Global NEST Journal **19** (2017) 269. https://doi.org/10.30955/gnj.001708.

[71] S. A. Adesokan, A. A. Giwa & I. A. Bello, "Removal of Trimethoprim from Water using Carbonized Wood Waste as Adsorbents", Journal of the Nigerian Society of Physical Sciences **3** (2021) 344. https://doi.org/10.46481/jnsps.2021.320.